A THREE DIMENSIONAL INVESTIGATION INTO THE ACOUSTIC PERFORMANCE OF DISSIPATIVE SPLITTER SILENCERS

Ray Kirby*

School of Engineering and Design,

Mechanical Engineering,

Brunel University,

Uxbridge, Middlesex, UB8 3PH, UK.

ray.kirby@brunel.ac.uk

Paul T. Williams

School of Engineering and Design,

Mechanical Engineering,

Brunel University,

Uxbridge, Middlesex, UB8 3PH, UK.

James Hill

AAF Ltd.,

Bassington Lane,

Cramlington,

Northumberland, NE23 8AF, UK.

Keywords: dissipative silencers, point collocation, insertion loss

Running Title: Three dimensional splitter silencers

* Corresponding author

ABSTRACT

Splitter silencers are found in ventilation and gas turbine systems and they normally consist of uniform sections of porous material aligned in parallel section that split the mean gas flowing within a duct. Theoretical investigations into dissipative splitter silencers have generally been limited to two dimensions and this restricts the analysis either to computing the silencer eigenmodes or, for a finite length silencer, to the analysis of a parallel baffle design provided it is excited by a plane wave. In this article a numerical point collocation approach is used to extend theoretical predictions to three dimensions. This facilitates the analysis of more complex silencer designs such as a "bar" silencer and new theoretical predictions are validated first by comparison with experimental measurements. The insertion loss of different silencer designs is then calculated and the performance of a bar silencer is compared to that of a traditional parallel baffle design for rectangular and circular ducts. It is shown here that a bar silencer with a volume of material identical to an equivalent parallel baffle design delivers a significant improvement in insertion loss at higher frequencies, although this is at the expense of a small reduction in performance at low frequencies.

I. INTRODUCTION

Dissipative silencers play an important role in attenuating broadband noise in ventilation systems and gas turbines. Understanding the performance of these so-called splitter silencers is important if one is to optimise silencer designs and successfully attenuate sound over a wide frequency range. Theoretical approaches for modelling splitter silencers are, however, currently limited to two dimensions and to the computation of the silencer eigenmodes, although for a finite length silencer with parallel rectangular baffles it is possible to use a two dimensional approach if the incident sound field is planar. To overcome these limitations this article applies a three dimensional approach, which permits the study of more complex silencer geometries and so enables an investigation into the relative performance of different splitter silencer designs, some of which have not appeared before in the literature.

In ventilation and gas turbine systems the limited space available means that it is necessary to place baffles of material in the mean flow field, this splits the flow field and gives rise to the generic terminology "splitter silencer." Placing the silencer in the mean flow field helps to raise the attenuation of the silencer because of the reflections imparted by the silencer inlet and this can be a significant source of attenuation at low frequencies. Of course, the downside of using a splitter silencer is that they raise the fluid pressure loss over the silencer and so lower the efficiency of the noise generating device such as a fan or turbine. Nevertheless, this type of silencer design is now well established, although the design normally consists of either parallel rectangular baffles (Fig. 1a), or a circular pod design (Fig. 2a). Here a silencer with parallel rectangular baffles has been studied extensively in the literature, although theoretical models for this type of silencer have traditionally been based only on computing the silencer eigenmodes, particularly the least attenuated mode[1]. It is only relatively recently that more complete theoretical models have been developed, with the scattering at either end of the silencer

accounted for using either numerical[2] or analytic techniques[2,3]. Kirby[4] later added the influence of a faring at either end of the silencer, although this required an assumption that the fairing was flat. It has, however, been shown experimentally that silencer designs that depart from the traditional rectangular baffle design are capable of delivering an improvement in silencer performance, at least at higher frequencies. This effect was first reported by Nillson and Söderquist[5], who demonstrated that a so-called bar silencer was capable of very large improvements in performance when compared to a rectangular splitter silencer. Here, the bar silencer consists of baffles that are square in cross-section, which are then suspended over the cross section of the airway, see Fig. 1b. This type of silencer was later investigated theoretically and experimentally by Cummings and Astley[6], although they were unable to reach a definitive conclusion regarding the claims made by Nillson and Söderquist[5]. The theoretical investigation of Cummings and Astley[6] is, however, based on a numerical prediction of the attenuation of the least attenuated mode only. This neglects the contribution from other modes, as well as the scattering from either end of the silencer. Such an approach may be valid at low frequencies, but it is unlikely to provide a true reflection of silencer performance at higher frequencies, especially as the upper frequency limit of interest for dissipative silencer designs is normally 8-10 kHz. Cummings and Astley[6] noted the limitations of their model and, when combined with a limited set of experimental data, they were unable to reach definitive conclusions regarding the relative performance of the two types of silencer shown in Fig. 1. It is interesting also to note that the study of Cummings and Astley is the only one to study "bar" silencers theoretically and those questions raised by the original article of Nillson and Söderquist[5] remained to be fully addressed. That is, will a change in geometry, for a fixed volume of absorbing material, deliver an improvement in performance when compared to a traditional parallel baffle design? This question can only be answered through the development of a three dimensional model and/or experimental measurements. However, three dimensional models are not well developed in the literature for this type of [bulk reacting] dissipative silencer. Here the only work of relevance is

the analytic study of Lawrie[7], who includes a bulk reacting material in a three dimensional model for a lined duct with a flexible wall. An analytic approach is suited to regular silencer geometries and here Lawrie placed a lining on opposite walls of a rectangular duct. It is, however, likely to be a considerable challenge to extend the analytic approach of Lawrie[7] to more complex silencer geometries such as a bar silencer and so it appears sensible here to move towards a numerical approach in which an arbitrary cross-sectional geometry may be accommodated.

The acoustic performance of dissipative silencers used in ventilation and gas turbine systems are normally quoted up to an octave band centre frequency of 8 kHz. This type of silencer may also be very large, with cross sectional dimensions of well over 1 m being common. It is not difficult to see that modelling this type of silencer presents a considerable computational challenge and it is only recently that computer hardware has advanced sufficiently to allow models for these silencers to be applied. Fortunately, the vast majority of commercial splitter silencers are uniform in the axial direction, apart from the fairing at either end of the silencer. This permits the use of modal solutions for the silencer section provided that one assumes that any geometrical non-uniformity in the fairings has a negligible impact on silencer performance. Accordingly, one may develop a three dimensional model through the use of two dimensional eigensolutions for the silencer section and the inlet/outlet ducts, and then joining the two regions through appropriate matching conditions. This article looks again at the performance of bar silencers, but this time accommodates the fairings at either end of the silencer, as well as all higher order modes that contribute to silencer performance. The performance of a bar silencer is then compared against a traditional rectangular baffled silencer and conclusions are drawn regarding their relative performance. Similarly, for a circular duct the performance of a pod silencer (Fig. 2a) is compared to an equivalent bar silencer for circular ducts (Fig. 2b). This is of interest as these silencer designs have yet to be studied in the literature using a comprehensive model of the type implemented here. A three dimensional finite element approach based on the point collocation

methodology of Kirby[4] is used to model silencer performance with a flat fairing at either end of the silencer. In view of the computational demands of a three dimensional model, mean flow is neglected from the results presented here. This is further justified on the basis that it is the relative performance of each silencer design that is of interest and that mean flow effects are likely to be consistent across each silencer design (with equivalent percentage open area). Moreover, for most splitter silencer applications mean flow values are modest in order to lower pressure losses over the silencer. To further validate the predictions presented here, comparisons will also be made with experimental measurements obtained according to ISO 7235[8]. The article begins in section II with a brief summary of the theoretical methodology; experimental measurements are discussed in section III, and in section IV experiment and theory are compared with one another and further theoretical investigations are undertaken regarding the relative performance of each silencer design.

II. THEORY

It was shown by Kirby[4] that the fairings at either end of a silencer should be included when modelling a silencer of finite length. The most computationally efficient way of including these fairings is to treat the silencer as uniform and to expand the pressure over the eigenmodes in each section of the silencer. If one assumes that these fairings may be treated as flat then continuity of pressure and velocity may be enforced over the discontinuities at each end of the silencer and a modal expansion retained on either side of each discontinuity. The most straightforward way to do this is through the use of point collocation, which is suited to enforcing the Neumann boundary conditions over both sides of the fairing. Thus, for silencers of arbitrary cross section point collocation is used here to enforce the continuity and boundary conditions over a two dimensional cross section. This method has been reported elsewhere for an elliptical automotive silencer,[9] and for a rectangular splitter

silencer[2,4], and the reader is referred to those other articles for a more complete description. With reference to Fig. 3, the acoustic wave equation for region q ($q = 1, 2, \mathrm{A}, \mathrm{M}$) is given by,

$$\frac{1}{c_q^2}\frac{\partial^2 p_q'}{\partial t^2} - \nabla^2 p_q' = 0, \tag{1}$$

where c_q is the speed of sound, p' is the acoustic pressure, and t is time. The acoustic pressure field in each region is expanded as an infinite sum over the duct eigenmodes to give

$$p_1'(x,y,z) = \sum_{m=0}^{\infty} \mathrm{F}_m \Phi_m(x,y) \mathrm{e}^{-\mathrm{i}k_0\gamma_m z_1} + \sum_{m=0}^{\infty} \mathrm{A}_m \Phi_m(x,y) \mathrm{e}^{\mathrm{i}k_0\gamma_m z_1} \tag{2}$$

$$p_\mathrm{s}'(x,y,z) = \sum_{m=0}^{\infty} \mathrm{B}_m \Psi_m(x,y) \mathrm{e}^{-\mathrm{i}k_0\lambda_m z_1} + \sum_{m=0}^{\infty} \mathrm{C}_m \Psi_m(x,y) \mathrm{e}^{\mathrm{i}k_0\lambda_m z_1} \tag{3}$$

$$p_2'(x,y,z) = \sum_{m=0}^{\infty} \mathrm{D}_m \Phi_m(x,y) \mathrm{e}^{-\mathrm{i}k_0\gamma_m z_2} \tag{4}$$

Here, F, A, B, C and D are the modal amplitudes, with the amplitude of the reflected modes in region R_2 set equal to zero (anechoic termination). For the inlet and outlet ducts, γ is the (dimensionless) axial wavenumber and $\Phi(\mathrm{x}, y)$ is the transverse duct eigenfunction, assuming that regions R_1 and R_2 are equal. For the silencer, λ is the (dimensionless) axial wavenumber and $\Psi(\mathrm{x}, y)$ is the eigenfunction for the region $R_s = R_\mathrm{A} + R_\mathrm{M}$. In addition, $k_0 = \omega/c_0$, where ω is the radian frequency and c_0 is the adiabatic speed of sound, with $\mathrm{i} = \sqrt{-1}$ and a time dependence of $\mathrm{e}^{\mathrm{i}\omega t}$ is assumed where $t = \mathrm{time}$.

In order to accommodate an arbitrary silencer cross-section it is necessary to use a numerical method and here the finite element method is used with each eigenfunction being approximated with a trial solution so that $\Phi = \mathbf{N}\boldsymbol{\Phi}$ and $\Psi = \mathbf{N}\boldsymbol{\Psi}$, where $\mathbf{N}$ is a global trial (or shape) function, and $\boldsymbol{\Phi}$ and $\boldsymbol{\Psi}$ hold the values of Φ and Ψ at each node in the finite element mesh. Following substitution of the expanded pressure into the acoustic wave equation and discretising the duct eigenfunctions one may construct a finite element eigenproblem for each region. In order to arrive at the final eigenequation it is necessary also to assign the transverse boundary conditions and here the duct walls are assumed to be rigid and impervious to sound. At the interface between the airway (A) and the absorbing material (M) it is assumed that a perforate is present so that the following boundary conditions apply [9]

$$\mathbf{u}_{\mathrm{A}} \cdot \mathbf{n}_{\mathrm{A}} = -\mathbf{u}_{\mathrm{M}} \cdot \mathbf{n}_{\mathrm{M}}, \tag{5}$$

and

$$p'_{\mathrm{A}} - p'_{\mathrm{M}} = \rho_0 c_0 \zeta \, \mathbf{u}_{\mathrm{M}} \cdot \mathbf{n}_{\mathrm{M}}, \tag{6}$$

where the fluid density in region $\mathrm{R_A}$ is ρ_0, $\mathbf{u}$ is the acoustic velocity vector and $\mathbf{n}$ is an (outward) unit normal. The (dimensionless) acoustic impedance of the perforate screen separating regions $\mathrm{R_A}$ and $\mathrm{R_M}$ is denoted ζ. Note that in order to enforce the pressure matching condition in Eq. (6) it is necessary to introduce (n_p) additional nodes so that two nodes sits on either side of the perforate and these are located adjacent to one another.

Following the derivation reported by Kirby[10], one may write a final eigenequation of the form

$$[\mathbf{R}_1 + \lambda^2 \mathbf{R}_3]\boldsymbol{\Psi} = \mathbf{0}, \tag{7}$$

where $\boldsymbol{\Psi} = [\boldsymbol{\Psi}_\mathrm{A} \quad \boldsymbol{\Psi}_\mathrm{M}]^\mathrm{T}$ and $\boldsymbol{\Psi}_\mathrm{A}$ and $\boldsymbol{\Psi}_\mathrm{M}$ are the values of the silencer eigenfunction in the airway and the porous material, respectively. The matrices in Eq. (7) are given as

$$\mathbf{R}_1\boldsymbol{\Psi} = [\mathbf{H}_\mathrm{A} - k_0^2\mathbf{L}_A]\boldsymbol{\Psi}_\mathrm{A} + \hat{\rho}^{-1}[\mathbf{H}_\mathrm{M} + \Gamma^2\mathbf{L}_\mathrm{M}]\boldsymbol{\Psi}_\mathrm{M} + (\mathrm{i}k_0/\zeta)[\mathbf{L}_\mathrm{pM} - \mathbf{L}_\mathrm{pA}]\{\boldsymbol{\Psi}_\mathrm{pM} - \boldsymbol{\Psi}_\mathrm{pA}\} \tag{8}$$

and

$$\mathbf{R}_3\boldsymbol{\Psi} = k_0^2\mathbf{H}_\mathrm{A}\boldsymbol{\Psi}_\mathrm{A} + \hat{\rho}^{-1}k_0^2\mathbf{H}_\mathrm{M}\boldsymbol{\Psi}_\mathrm{M} \tag{9}$$

with the finite element matrices for element shape function N are given as

$$\mathbf{H}_\mathrm{A,M} = \int_{\mathrm{R_{A,M}}} \nabla\mathrm{N}^\mathrm{T} \cdot \nabla\mathrm{N}\ dxdy, \tag{10}$$

$$\mathbf{L}_\mathrm{A,M} = \int_{\mathrm{R_{A,M}}} \mathrm{N}^\mathrm{T}\mathrm{N}\ dxdy, \tag{11}$$

$$\mathbf{L}_\mathrm{pA,M} = \int_{\mathrm{S_{pA,M}}} \mathrm{N}^\mathrm{T}\mathrm{N}\ dxdy. \tag{12}$$

Here vectors $\boldsymbol{\Psi}_\mathrm{pA}$ and $\boldsymbol{\Psi}_\mathrm{pM}$ hold values of $\boldsymbol{\Psi}$ on the perforated screen, and $\mathrm{S_{pA}}$ and $\mathrm{S_{pM}}$ denote the surface of the perforated sheet lying in regions $\mathrm{R_A}$ and $\mathrm{R_M}$, respectively. For region $\mathrm{R_M}$, the propagation constant of the porous material is denoted by Γ and the equivalent complex density by $\rho(\omega)$, where $\hat{\rho} = \rho(\omega)/\rho$, see Kirby[4]. Equation (7) is solved for n_C eigenvalues and their associated eigenfunctions, where n_C is the number of nodes in the finite element mesh. A similar procedure is carried out for the empty ducts before and after the silencer, which delivers n_1 and n_2 eigensolutions, respectively, with $n_1 = n_2$ in the analysis that follows.

After obtaining the eigenvalues and eigenvectors for each region, continuity of pressure and normal particle velocity are enforced over planes S_1 and S_2, see Fig. 3. This is carried out using point collocation, which is potentially computationally slower than taking advantage of

modal orthogonality and matching velocity flux; however, it is difficult here to enforce zero normal velocity over both sides of a fairing using mode matching because for this type of problem a mode matching solution converges slowly. Thus, the point collocation approach is used here, although it is possible to economise on computational expenditure by using a smaller number of modes when compared to collocation points. Application of the axial matching conditions delivers the following system of equations:

$$\sum_{j=0}^{m_1} \mathrm{A}_j \boldsymbol{\Phi}_{\mathrm{A}j} - \sum_{j=0}^{m_c} \mathrm{B}_j \boldsymbol{\Psi}_{\mathrm{A}j} - \sum_{j=0}^{m_c} \tilde{\mathrm{C}}_j \boldsymbol{\Psi}_{\mathrm{A}j}\, e^{-\mathrm{i}k_0\lambda_j L} = -\mathrm{F}_0 \boldsymbol{\Phi}_{\mathrm{A}0} \tag{13}$$

$$\sum_{j=0}^{m_c} \mathrm{B}_j \boldsymbol{\Psi}_{\mathrm{A}j}\, e^{-\mathrm{i}k_0\lambda_j L} + \sum_{j=0}^{m_c} \tilde{\mathrm{C}}_j \boldsymbol{\Psi}_{\mathrm{A}j} - \sum_{j=0}^{m_1} \mathrm{D}_j \boldsymbol{\Phi}_{\mathrm{A}j} = 0 \tag{14}$$

$$\sum_{j=0}^{m_1} \mathrm{A}_j \gamma_{\mathrm{j}} \boldsymbol{\Phi}_{\mathrm{A}j} + \sum_{j=0}^{m_c} \mathrm{B}_j \lambda_{\mathrm{j}} \boldsymbol{\Psi}_{\mathrm{A}j} - \sum_{j=0}^{m_c} \tilde{\mathrm{C}}_j \lambda_{\mathrm{j}} \boldsymbol{\Psi}_{\mathrm{A}j}\, e^{-\mathrm{i}k_0\lambda_j L} = -\mathrm{F}_0 \gamma_0 \boldsymbol{\Phi}_{\mathrm{A}0} \tag{15}$$

$$\sum_{j=0}^{m_c} \mathrm{B}_j \lambda_{\mathrm{j}} \boldsymbol{\Psi}_{\mathrm{A}j}\, e^{-\mathrm{i}k_0\lambda_j L} + \sum_{j=0}^{m_c} \tilde{\mathrm{C}}_j \lambda_{\mathrm{j}} \boldsymbol{\Psi}_{\mathrm{A}j} - \sum_{j=0}^{m_1} \mathrm{D}_j \gamma_{\mathrm{j}} \boldsymbol{\Phi}_{\mathrm{A}j} = 0 \tag{16}$$

$$\sum_{j=0}^{m_c} \mathrm{B}_j \lambda_{\mathrm{j}} \boldsymbol{\Psi}_{\mathrm{M}j} - \sum_{j=0}^{m_c} \tilde{\mathrm{C}}_j \lambda_{\mathrm{j}} \boldsymbol{\Psi}_{\mathrm{M}j} e^{-\mathrm{i}k_0\lambda_j L} = 0 \tag{17}$$

$$\sum_{j=0}^{m_c} \mathrm{B}_j \lambda_{\mathrm{j}} \boldsymbol{\Psi}_{\mathrm{M}j}\, e^{-\mathrm{i}k_0\lambda_j L} - \sum_{j=0}^{m_c} \tilde{\mathrm{C}}_j \lambda_{\mathrm{j}} \boldsymbol{\Psi}_{\mathrm{M}j} = 0 \tag{18}$$

$$\sum_{j=0}^{m_1} \mathrm{A}_j \gamma_\mathrm{j} \boldsymbol{\Phi}_{\mathrm{A}j} = \mathrm{F}_0 \gamma_0 \boldsymbol{\Phi}_{\mathrm{A}0} \tag{19}$$

$$\sum_{j=0}^{m_1} \mathrm{D}_j \gamma_\mathrm{j} \boldsymbol{\Phi}_{\mathrm{M}j} = 0. \tag{20}$$

Here $\tilde{\mathrm{C}}_j = \mathrm{C}_j e^{\mathrm{i}k_0 \lambda_j L}$, where L is the length of the silencer. Equations (13) and (14) match pressure, whilst (15) and (16) match axial velocity over planes S_1 and S_2,, respectively. This makes use of m_1 eigenfunctions for $\boldsymbol{\Phi}_\mathrm{A}$ and m_c eigenfunctions for $\boldsymbol{\Psi}_\mathrm{A}$. Note that the length of the (column) vectors $\boldsymbol{\Phi}_\mathrm{A}$ and $\boldsymbol{\Psi}_\mathrm{A}$ is n_A, where n_A is the number of collocation points in region $\mathrm{R_A}$, with $m_1 \leq n_1$. Equations (17) and (18) enforce zero axial velocity over the fairings in region $\mathrm{R_s}$, over planes S_1 and S_2, respectively. Here the number of nodes in region $\mathrm{R_m}$ is denoted by n_M, so that the length of the column vectors $\boldsymbol{\Phi}_\mathrm{M}$ and $\boldsymbol{\Psi}_\mathrm{M}$ is n_M. This gives a total number of collocation points in region $\mathrm{R_s}$ equal to $n_\mathrm{c} = n_\mathrm{A} + n_\mathrm{M}$. For the surface of the fairings that lie in regions $\mathrm{R_1}$ and $\mathrm{R_2}$, zero axial velocity is enforced using Eqs. (19) and (20), respectively. Here, the length of the column vector $\boldsymbol{\Phi}_\mathrm{A}$ is equal to the number of collocation points, $n_c - n_\mathrm{P}$, so that matching takes place over n_P fewer collocation points in regions $\mathrm{R_1}$ and $\mathrm{R_2}$ when compared to $\mathrm{R_c}$. Thus, Eqs. (13) to (20) deliver $2(n_\mathrm{A} + n_\mathrm{M} + n_1)$ collocation points, with $2(m_1 + m_\mathrm{c})$ unknown modal amplitudes. This system of equations may be solved provided $m_1 + m_\mathrm{c} \leq n_\mathrm{A} + n_\mathrm{M} + n_1$, assuming plane wave excitation so that $\mathrm{F}_0 = 1$. Note that one may choose to solve the problem with $m_1 + m_\mathrm{c} < n_\mathrm{A} + n_\mathrm{M} + n_1$ so that the number of collocation points exceeds the number of modal amplitudes. This delivers an overdetemined system matrix, which may be solved using, for example, a numerical least squares based approach. Finally, the transmission loss (TL) of the silencer is defined as the ratio of the transmitted to incident sound power, so that

$$\mathrm{TL} = -10\ \log_{10} \sum_{j=0}^{n_I} \frac{\gamma_j I_j \left|\mathrm{D_j}\right|^2}{I_0}, \tag{21}$$

where $I_j = \int_{\mathrm{R_1}} \left|\Phi_j(\mathrm{x}, y)\right|^2 dxdy$, and n_I is the number of propagating modes in region $\mathrm{R_2}$.

III. EXPERIMENT

Experimental measurements are used here to validate the theoretical model, as well as providing evidence to support the investigation into the relative performance of different silencer designs. There are two international standards outlining a methodology for measuring silencer insertion loss, the European standard EN ISO 7235[8] and the U.S. standard ASTM E477[12]. The two standards attempt to measure the insertion loss (IL) of a silencer and it is assumed in both standards that this is equivalent to the silencer TL obtained in the previous section. There are a number of differences between the standards, although the only significant difference appears to be the addition of a "modal filter" in the ISO 7235 standard. Here the European standard requires the placement of an additional silencer, or modal filter, between the sound source and the silencer test section. The purpose of this filter is to damp down high order propagating modes generated by the sound source so that the sound field incident on the test silencer is predominantly planar. This is intended to deliver plane wave excitation across the frequency spectrum, as well as decoupling the sound source from the test silencer. It is debatable how well this will work in practice, especially at relatively high frequencies, however it is possible that this approach will help to standardise tests over different test facilities. This is because the IL tests should be, as far as possible, independent of the characteristics of the sound source and it is likely that the modal filter will go some way towards achieving this. Evidence for the repeatability of tests over different facilities

when using ISO 7235[8] is provided by Hill et al.[13] Furthermore, there is some evidence that when using the U.S. standard it is more difficult to deliver repeatability over different test facilities[14,15], and it is possible that this is caused by the absence of a modal filter in the U.S. standard. Of course, the disadvantage of using a modal filter is that it lowers the incident sound pressure level and this may cause problems with the measured signal to noise ratio, especially when mean flow is present. However, the results presented here do not include mean flow so this is unlikely to cause problems with the signal to noise ratio in the current tests. Furthermore, there are significant advantages to specifying an incident plane wave when comparing measurement against prediction as this unambiguously defines the incident sound field in the theoretical model. Therefore, the European ISO 7235[8] standard is adopted here when measuring silencer IL, with a reverberation room used downstream of the silencer in order to measure the transmitted sound power. For reasons of brevity the details of this test rig are not discussed further here and instead the reader is referred to ISO 7235[8], although it is noted that all of the commissioning tests specified by the standard have been carried out so that the requirements of this standard have been met in full. Further details are discussed by Hill et al.[13], where it is also demonstrated that the tests carried out using this facility compare very well with separate tests undertaken on an independent test facility also built according to ISO 7235. Four different silencer designs are measured here, with the acronym SDM referring to a parallel baffled rectangular silencer (Fig. 1a); MDM refers to a rectangular "bar" silencer (Fig. 1b); TDM refers to a pod silencer (Fig. 2a); and CMDM refers to a circular "bar" silencer (Fig. 2b). Note here that for the MDM and CMDM silencers some extra support is required to hold the "bars" in place; this supporting structure is assumed to be sufficiently thin so that it does not influence the sound propagation and may be neglected in the theoretical model. The silencers measured experimentally are SDM 1,

TDM 1, MDM 1, and CMDM 1; the geometry of these silencers is listed in Tables I and II. Note that for the CMDM silencers the centre "bars" are either square, or isosceles triangles.

The theoretical model requires the bulk acoustic properties of the porous material to be specified and these were measured using an impedance tube and the two microphone technique[16]. The properties are then expressed using Delany and Bazley coefficients[17], so that

$$\Gamma/k_0 = 0.2722\xi^{-0.4718} + \mathrm{i}[1 + 0.2432\xi^{-0.4326}], \tag{22}$$

and for the normalised complex density

$$\hat{\rho} = -(\Gamma/k_0)\{0.1591\xi^{-0.5328} + \mathrm{i}[1 + 0.1316\xi^{-0.5391}]\}. \tag{23}$$

Here $\xi = \rho f/\Theta$, where f is frequency and Θ is the flow resistivity of the porous material. Following previous articles by the first author, a semi-empirical correction is used here to avoid inconsistencies in the Delany and Bazley curve fitting formulae at low frequencies[4,18]. This yields a value of 3.63 for the steady flow tortuosity at a transition value of $\xi = 0.0056$. For the perforated screen that lies between the airway and the rock wool, the semi-empirical model of Kirby and Cummings is used[19]. This model is further modified using the method suggested by Denia et al.[20], to give

$$\zeta = [\zeta' + \mathrm{i}0.425kd(\hat{\rho} - 1)\mathrm{F}(\sigma)]/\sigma, \tag{24}$$

with

$$\mathrm{F}(\sigma) = 1 - 1.06\sigma^{0.5} + 0.17\sigma^{1.5}. \tag{25}$$

Here, σ is the open area porosity of the perforated screen, d is the hole diameter and ζ' is the orifice impedance measured in the absence of a porous material. Values for ζ' are widely available in the literature, although the data measured by Kirby and Cummings[19] is used here. For each silencer studied, $d = 3$ mm, $\sigma = 27\%$ and the thickness of the perforated screen $t = 1.6$ mm.

IV. RESULTS AND DISCUSSION

The validity of the numerical model is investigated first by comparing predictions against the experimental measurements obtained according to ISO 7235[8]. In Fig. 4 the predicted and measured IL is presented for the SDM 1 silencer using one third octave frequency bands. For the SDM 1 silencer plane wave excitation means that it is possible to use a two dimensional theoretical analysis and here 296 degrees of freedom were required, with $n_c = 75$, $n_A = 73$ (and using $m_1 = n_1$, $m_c = n_c$). Clearly, for a two dimensional problem the degrees of freedom required are relatively low and so one may obtain solutions quickly, even for a large frequency range. It is evident in Fig. 4 that good agreement between prediction and measurement is possible, at least for this silencer design. Here, the model has successfully captured silencer performance at low and high frequencies, with only a slight over prediction of peak silencer performance. This agreement between prediction and measurement for a silencer with parallel baffles represents an improvement on that seen previously in the literature for parallel baffles[4,21]. However, it is noted here that this silencer has a relatively high open area of $\Delta = 50\%$, whereas those problems identified previously when comparing prediction and experiment are generally found at lower percentage open areas. Further tests indicate that the model is capable of successfully capturing SDM silencer performance over a wide frequency range for $\Delta \geq 35\%$. For lower percentage open areas some over prediction

of silencer performance is observed at higher frequencies. In Fig. 5 the theoretical model is compared against measurement for a TDM silencer, which is sometimes called a "pod" silencer, see for example the plane wave analysis of Munjal[22]. This type of silencer is the circular equivalent of the SDM silencer seen in the previous example and so again it is only necessary to generate a two dimensional model, and here 328 degrees of freedom were used. A comparison between prediction and measurement in Fig. 5 shows a level of agreement comparable to that seen for the SDM silencer in Fig. 4. Again, the low and high frequency behaviour is fully captured and one sees a small over prediction in silencer performance in the mid frequency range. Note that for the pod silencer, the outer lining forms an expansion chamber so that the inlet and outlet ducts have a radius of $a + b$. This means that there is some ambiguity over how to define the percentage open area of a pod silencer. The definition used here includes the outer lining so that for SDM 1, $\Delta = 23.6\%$; if the outer lining is not included then $\Delta = 44.6\%$.

The MDM and CMDM silencer designs (Figs. 1b and 2b) require a three dimensional model, although it is still possible to take advantage of symmetry if the silencer is excited by a plane wave. For example, if an MDM silencer has four "bars" arranged symmetrically then it is necessary to mesh only one quarter of the silencer. This requires 2,052 degrees of freedom for the MDM 1 silencer and solution times were approximately 15 times that seen for the SDM 1 silencer. It is possible to lower this solution time by taking fewer modes than collocation points and it was found that this generally works well at low frequencies so that one can successfully obtain accurate IL predictions using about 30% of the modes computed in the eigenvalue analysis; however, once the frequency increases above the first cut on mode in the inlet/outlet ducts then the number of modes must be increased steadily so that when one reaches frequencies above about 4 kHz it is necessary to have the number of modes equal

to the number of collocation points in order to maintain accuracy. Thus, by varying the number of modes included in the analysis one may readily implement an adaptive approach for the final system matrix, which works like the usual finite element approach of adapting the number of elements to accommodate a change in frequency. However, the advantage of changing the number of modes used in the collocation procedure is that one does not need to re-mesh at every frequency.

A comparison between prediction and measurement in Fig. 6 shows that generally good agreement can be maintained at low and high frequencies, although at medium to high frequencies some over prediction is evident. This type of over prediction has been observed before for SDM silencers of low percentage open areas[4,22]. It is not entirely clear why this discrepancy exists for SDM silencers and also for the MDM silencer seen in Fig. 6; it has been speculated previously[4] that this may be caused by sound travelling down the walls of the silencer during experimental measurements. However, further investigation aimed at eliminating the possibility of flanking noise transmission suggests that this may not be the reason for this discrepancy. Other possible reasons include: (i) inaccuracies in the theoretical model, for example when quantifying the performance of the material and/or the behaviour of the perforated screen under multi-modal conditions; or (ii) inaccuracies in the experimental measurements caused by, for example, the assumption that IL and TL measurements are equivalent to one another. This latter point depends on the impedance of the sound source being the same for separate tests undertaken with and without the silencer in place, and it is thought that this assumption may be less appropriate when, for example, the percentage open area of the silencer is reduced because it reflects more energy back towards the source.

In Fig. 7 a circular equivalent of the MDM design is investigated, which is called here a CMDM silencer (see Fig. 2b). The circular geometry delivers a more complex silencer design than that seen for the MDM silencer, although it is still possible to model only one quarter of the silencer cross-section. For this silencer 2,642 degrees of freedom were used which took approximately 25 times longer that the TDM silencer to solve for the full frequency range. Comparison between prediction and measurement in Fig. 7 is generally good and here it is seen that better agreement is achieved at higher frequencies, although it is noted that a small overprediction appears at lower frequencies but this is generally within experimental uncertainty. A comparison between prediction and measurement for the four different silencer designs demonstrates that the theoretical models are generally capable of capturing silencer performance over a wide frequency range, although some over prediction is evident for the MDM silencer at higher frequencies. It does, however, appear reasonable to conclude here that the theoretical model is capable of delivering a good quantitative guide to actual silencer performance. Accordingly, it appears justifiable to use this model to investigate and to compare the relative performance of different silencer designs.

It is interesting first to investigate the observations of Cummings and Astley[6] with regards to the relative performance of the SDM and MDM silencers. In Fig. 8 the predicted insertion loss of the first silencer studied by Cummings and Astley is shown, so that these values are to be compared with the data presented in Fig. 4 of ref. 6. Here, a porous material with uniform properties is assumed with a representative flow resistivity of $\Theta = 19{,}307$ N s/m^4 and the Delany and Bazley coefficients reported for rock wool in Eqs. (22) and (23) are used. The dimensions of the SDM silencer used by Cummings and Astley are $a = 0.1333$ m, $b = 0.1667$ m, and $L = 2$ m; for the MDM silencer $d_x = d_y = 0.4$ m, $e_x = e_y = 0.1$ m, and $L = 2$ m. Cummings and Astley[6] suggest that in order to deliver a fair comparison between the

two different silencer designs one should equate percentage open area and hydraulic diameter; however, for plane wave excitation the hydraulic diameter is meaningless for the SDM silencer because silencer performance is independent of silencer height[2]. Accordingly, a percentage open area of $\Delta = 55.55\%$ is maintained for the two silencers designs and a comparison between the IL predictions in Fig. 8 shows a clear improvement in performance delivered by the MDM silencer at medium and high frequencies, with a small reduction in performance at lower frequencies. This supports the observations of Nillson and Söderquist[5]. In order to further explore the observations of Cummings and Astley[6], Fig. 8 also presents the attenuation (in dB/m) of the least attenuated mode for each silencer and here it is evident that the behaviour of the least attenuated mode is different from the IL. At higher frequencies the attenuation of the least attenuated mode is very similar for both silencers, and this is why Cummings and Astley concluded that there was little evidence of a difference in performance between the two designs at higher frequencies. Moreover, Cummings and Astley were able to generate predictions at high frequencies only for those silencers with a relatively high percentage open area; for lower percentage open areas their predictions do not go beyond the mid frequency range. It will be seen in later figures that for higher percentage open areas the effect of a change in design is reduced so that Cummings and Astley have missed significant differences in performance because their model was unable to cover a wide frequency range for lower percentage open areas. Accordingly, it is not surprising that Cummings and Astley were unable to deduce a change in performance between the two designs given the limitations of their theoretical model. In their conclusions Cummings and Astley note these limitations and because of this they do not commit to definitive conclusions. The results presented here demonstrate that one can only resolve this issue using a three dimensional theoretical model for IL, and that the MDM silencer will improve high frequency performance when compared to an SDM silencer of equivalent open area. When comparing the relative performance of

each silencer Nillson and Söderquist[5] speculated upon the reasons for the improvement in silencer performance; Cummings and Astley[6] later reviewed this analysis and concluded that arguments based upon "constriction" and "diagonal" effects in the MDM silencer were of limited use. Moreover, it can be concluded here that this increase in performance is not caused by an increase in the length of the perimeter of the material exposed to the flow; this is because the performance of the SDM silencer is independent of silencer height. The possible reasons behind this change in performance will be explored further on in this section following the generation of additional silencer data.

It is interesting to see if the improvements observed in Fig. 8 hold more generally. Accordingly, the relative performance of each design is investigated with respect to the percentage open area of the silencer and this is carried out here for percentage open areas of 75% (silencer 2), 50% (silencer 3) and 25% (silencer 4). IL predictions are presented in Figs. 9a-c for the SDM and MDM silencers, and Figs. 10a-c for the TDM and CMDM silencer, see also Tables I and II for the geometries of these silencers. Here, the volume of material in those silencers being compared to one another is kept constant, as is the silencer length and the material flow resistivity. It is evident in Figs, 9a-c that an MDM silencer always performs better than an SDM silencer at higher frequencies, whereas at low frequencies a small reduction in performance is observed. Moreover, the advantages gained from arranging the material in an MDM formation increases as the percentage open area decreases, although at low percentage open areas the predicted silencer IL becomes very large and this would not be realised in practice, as breakout noise and other flanking paths would compromise silencer performance. In Figs. 10a-c the relative performance of the circular silencers is seen to be similar to that of the rectangular silencers, although an even larger increase in performance for the CMDM silencers is observed at higher frequencies. Thus, the results presented in

Figs. 9 and 10 clearly illustrate that improvements in performance may be achieved if one re-designs the silencer geometry and this further supports the original observations of Nillson and Söderquist[5].

In the examples shown here only four "bars" were used for the MDM silencer and six for the CMDM silencer. If one increases the number to, say, 16 for the MDM silencer, then a significant further increase in IL is achieved at higher frequencies, although this is at the expense of a reduction in low frequency performance. This is also observed for the CMDM silencers. Thus, the general principle behind the observations of Nillson and Söderquist[5] are true even if one continues to split the silencer up into ever smaller "bars". Obviously, there is a practical limit to how far one can go with such an approach, both in terms of silencer production costs and mechanical design, but also the reduction in low frequency performance, which is an area that is often very important in commercial applications. However the general principle observed by Nillson and Söderquist[5] that by reducing the gap between the silencer elements (by continuously splitting up the material) will improve silencer performance. Furthermore, the open area of the silencer represents the most significant parameter when it comes to observing a difference in performance between the two different silencer designs. Changes in material flow resistivity will of course change the individual performance of a silencer, but the relative performance of each type of silencer generally follows the behaviour observed in Figs. 9 and 10 so that the MDM and CMDM will continue to deliver increased performance at higher frequencies.

The results presented in Figs. 8 – 10 clearly demonstrate that arranging the absorbing material in the form of discrete "bars" will improve silencer performance. It is proposed here that the reason for this improvement in performance is twofold: (i) the attenuation of the least

attenuated mode is increased at higher frequencies because the incident plane wave finds it easier to penetrate a material arranged in a series of "bars"; and (ii) that the higher order modes in the MDM/CMDM silencers are significantly less attenuated than for the SDM/TDM silencers and this facilitates the transfer of energy from the incident plane wave into these higher order modes. This is illustrated in Fig. 11, where the attenuation of the first five least attenuated modes is presented for the SDM 4 and MDM 4 silencers. Here, one can see that for the MDM silencer the attenuation of the least attenuated mode is significantly higher than for the SDM silencer, and for the higher order modes their attenuation is significantly lower. Accordingly, it is likely that this will facilitate stronger coupling between the incident sound field and the modes inside the MDM silencer. This coupling will transfer more energy into the higher order modes and because these are, by definition, more highly attenuated than the least attenuated mode, any energy transferred to these modes will serve to increase overall silencer attenuation. Further evidence for this was observed in the modal amplitudes for the higher modes in the MDM silencer, which are higher than the equivalent values seen in the SDM silencer. Accordingly, if one wishes to improve silencer performance, at least in the high frequency range, then one should aim to lower the attenuation of the higher order modes, as well as increase the attenuation of the least attenuated mode. Arranging the material in the form of bars appears to help in achieving this goal. However, it is thought that any further changes to, say, the MDM geometry are unlikely to deliver a significant improvement over and above that seen here, and that any further refinement of the geometry may incur a disproportionate increase in the cost of fabricating the silencer.

V. CONCLUSIONS

This article describes a theoretical methodology suitable for accommodating three dimensional behaviour in dissipative splitter silencers. This approach permits the inclusion of higher order modes in the silencer section, as well as the scattering of higher order modes by fairings at the inlet and outlet of the silencer. Through the use of point collocation it is shown that silencer end effects may also be included so that the three dimensional characteristics of a finite length silencer may be analysed. This then permits the study of new silencer designs and delivers answers to questions previously raised in the literature about the relative performance of different designs. The theoretical model is validated by comparing predictions against experimental measurements obtaining according to ISO 7235[8]. Here generally good agreement between prediction and experiment is observed for four different silencer designs over a frequency range of 25 Hz to 8 kHz. It is, however, evident that some over prediction of silencer performance occurs for the MDM silencer at higher frequencies. Nevertheless it is concluded that the theoretical model is generally capable of capturing the performance of a splitter silencer, including those silencers in which three dimensional behaviour is present. That is, the accuracy of the theoretical model is not compromised by moving from two to three dimensions.

A three dimensional model permits an investigation into the relative performance of two different silencer designs and a traditional parallel baffle design was compared to a silencer in which the material is arranged as a series of “bricks” or “bars”. These two designs have been studied previously in the literature, where there was some debate regarding what is the most effective of the two designs. The results presented here demonstrate that a bar type silencer is significantly more effective in attenuating sound at high frequencies, whereas at low

frequencies the parallel baffle silencer delivers the better performance. This supports the original findings of Nillson and Söderquist[5] and here one may conclude that for a given volume of material it is more effective to arrange the silencer material as a series of "bars" provided one can tolerate a small drop in performance at low frequencies. This behaviour is also demonstrated for an equivalent circular design, which further illustrates the general philosophy that the splitting up of material into ever smaller sections will increase high frequency performance at the expense of a small drop in low frequency performance. It was also shown that the difference in performance between the two designs is influenced by the percentage open area of the silencer, so that the most significant change in silencer performance was observed for those silencers with a low percentage open area.

A three dimensional model has been shown here to be capable of delivering insights into the relative performance of different silencer geometries. It is proposed that this change in performance is caused by higher order modes in a bar silencer coupling more readily to the incident sound field when compared to a parallel baffled silencer. However, new designs that seek to further take advantage of this effect may incur additional manufacturing costs and this may in the future place a limit on the number of sections, or bars, that can be accommodated. Moreover, it is common for the low frequency performance of a silencer to be very important in many installations and the results presented here demonstrate that any modification of silencer design must be carefully considered so as not to unduly compromise low frequency performance.

ACKOWLEDGEMENTS

The authors would like to thank the UK Technology Strategy Board (TSB), through the Knowledge Transfer Programme (KTP), for their support of the work reported in this article.

REFERENCES

1. A. Cummings, N. Sormaz, Acoustic attenuation in dissipative splitter silencers containing mean fluid flow, *Journal of Sound and Vibration* 168, 209-227 (1993).
2. R. Kirby, J.B. Lawrie, A point collocation approach to modelling large dissipative silencers, *Journal of Sound and Vibration* 286 (2005) 313-339.
3. J.B. Lawrie, R. Kirby, Mode matching without root finding: Application to a dissipative silencer, *Journal of the Acoustical Society of America*, 119, 2006, 2050-2061.
4. R. Kirby, "The influence of baffle fairings on the acoustic performance of rectangular splitter silencers," *Journal of the Acoustical Society of America*, 118, 2005, 2302-2312.
5. N-Å. Nilsson, S. Söderqvist, "The bar silencer – improving attenuation by constricted two-dimensional wave propagation," Proceedings of Inter-Noise 83, 1983, 1-4.
6. A. Cummings and R.J. Astley, "Finite element computation of attenuation in bar-silencers and comparison with measured data," *Journal of Sound and Vibration* 196 (1996) 351-369.
7. J.B. Lawrie, "On acoustic propagation in three dimensional rectangular ducts with flexible walls and porous linings," *Journal of the Acoustical Society of America*, 131, 2012, 1890-1901.
8. European Standard EN ISO 7235, "Measurement procedures for ducted silencers – insertion loss, flow noise and total pressure loss," (2003).
9. R. Kirby, Transmission loss predictions for dissipative silencers of arbitrary cross section in the presence of mean flow, *Journal of the Acoustical Society of America* 114 (2003) 200-209.

10. R. Kirby, A comparison between analytic and numerical methods for modelling automotive dissipative silencers with mean flow, *Journal of Sound and Vibration* 325 (2009) 565-582.
11. R.J. Astley, A. Cummings, A finite element scheme for attenuation in ducts lined with porous material, *Journal of Sound and Vibration* 116 (1987) 239-263.
12. ASTM E477, "Standard Test Method for Measuring Acoustical and Airflow Performance of Duct Liner Materials and Prefabricated Silencers," DOI. 10.1520/E0477-06A.
13. J. Hill, P. Williams, D. Herries, An investigation into the effect of receiving side arrangements on measurements made in accordance with ISO 7235, *Proceedings of Euronoise 2012*, Prague (2012).
14. T. Paige, Wanted – New ideas for testing duct silencers, *AMCA International In Motion, Spring 2007*, 24-25.
15. J.G. Lilly, Suggested modifications to ASTM test method E477, *Sound and Vibration*, (June 2011) 14-15.
16. European Standard EN ISO 10534-2:2001, Determination of sound absorption coefficient and impedance in impedance tubes. Transfer function method. (2001).
17. M.E. Delany and E.N. Bazley, Acoustical properties of fibrous materials. *Applied Acoustics* 3 (1970) 105-116.
18. R. Kirby and A. Cummings, Prediction of the bulk acoustic properties of fibrous materials at low frequencies, *Applied Acoustics* **56**, 101-125 (1999).
19. F.D. Denia, A. Selamet, F.J. Fuenmayor and R. Kirby, Acoustic attenuation performance of perforated dissipative mufflers with empty inlet/outlet extensions, *Journal of Sound and Vibration* 302 (2007) 1000-1017.

20. R. Kirby and A. Cummings, The impedance of perforated plates subjected to grazing mean flow and backed by porous media, *Journal of Sound and Vibration* 217 (1998) 619-636.
21. F.P. Mechel, Numerical results to the theory of baffle-type silencers, *Acustica* 72, 7-20 (1990).
22. M.L. Munjal, "Analysis and design of pod silencers," *Journal of Sound and Vibration* 262 (2003) 497-507.

Table I. Geometries for SDM and TDM silencers

Silencer	a (m)	b (m)	t_l (m)	L (m)	Θ $\mathrm{N\,s/m^4}$	Δ (%)
SDM 1	0.100	0.100	-	1.8	1,881	50
SDM 2	0.150	0.050	-	0.9	44,691	75
SDM 3	0.100	0.100	-	0.9	44,691	50
SDM 4	0.050	0.150	-	0.9	44,691	25
TDM 1	0.291	0.100	0.147	0.9	27,868	23.6
TDM 2	0.088	0.303	0.050	0.9	38,520	75
TDM 3	0.191	0.200	0.147	0.9	38,520	40
TDM 4	0.272	0.119	0.147	0.9	38,520	25

Table II. Geometries for MDM and CMDM silencers

Silencer	d_x (m)	d_y (m)	e_x (m)	e_y (m)	r (m)	t_l (m)	L (m)	Θ N s/m^4	Δ (%)
MDM 1	0.280	0.210	0.060	0.045	-	-	0.9	19,307	51
MDM 2	0.198	0.148	0.101	0.076	-	-	0.9	44,691	75
MDM 3	0.280	0.210	0.060	0.045	-	-	0.9	44,691	50
MDM 4	0.345	0.275	0.285	0.022	-	-	0.9	44,691	25
CMDM 1	0.130	-	0.098	-	0.39	0.147	0.9	38,520	40
CMDM 2	0.185	-	0.056	-	0.39	0.05	0.9	38,520	75
CMDM 3	0.130	-	0.098	-	0.39	0.147	0.9	38,520	40
CMDM 4	0.056	-	0.098	-	0.39	0.147	0.9	38,520	25

Figure Captions

Figure 1a: Parallel baffle (SDM) splitter silencer

Figure 1b: Square “bar” (MDM) splitter silencer

Figure 2a: Circular “pod” (CDM) splitter silencer

Figure 2b: Circular “bar” (CMDM) splitter silencer

Figure 3. Geometry of uniform silencer.

Figure 4. Measured and predicted IL for silencer SDM 1. ———, prediction; ▲ , measurement.

Figure 5. Measured and predicted IL for silencer TDM 1. ———, prediction; ▲ , measurement.

Figure 6. Measured and predicted IL for silencer MDM 1. ———, prediction; ▲ , measurement.

Figure 7. Measured and predicted IL for silencer CMDM 1. ———, prediction; ▲ , measurement.

Figure 8. Predictions for Cummings and Astley silencer [16]. ———, IL SDM; ———, IL MDM; – – – – ·, attenuation SDM; ; — — —, attenuation MDM

Figure 9a. Predicted IL for Δ= 75%. ————, SDM 2; — — —, MDM 2 .

Figure 9b. Predicted IL for Δ= 50%. ————, SDM 3; — — —, MDM 3 .

Figure 9c. Predicted IL for Δ= 25%. ————, SDM 4; — — —, MDM 4 .

Figure 10a. Predicted IL for Δ= 75%. ————, TDM 2; — — —, CMDM 2 .

Figure 10b. Predicted IL for Δ= 40%. ————, TDM 3; — — —, CMDM 3 .

Figure 10c. Predicted IL for Δ= 25%. ————, TDM 4; — — —, CMDM 4 .

Figure 11. Predicted attenuation of the first five least attenuated modes.

————, SDM 4; — — —, MDM 4.

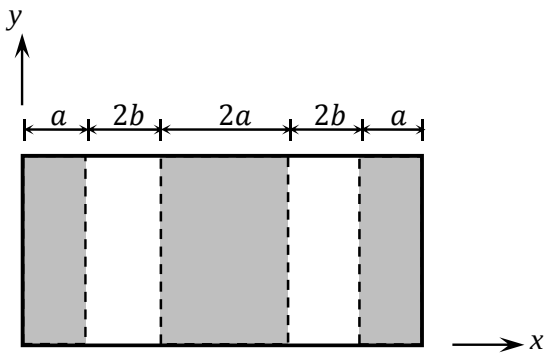

Figure 1a: Parallel baffle (SDM) splitter silencer

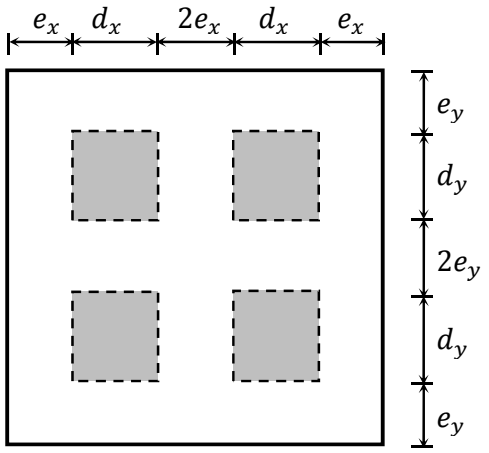

Figure 1b: Square “bar” (MDM) splitter silencer

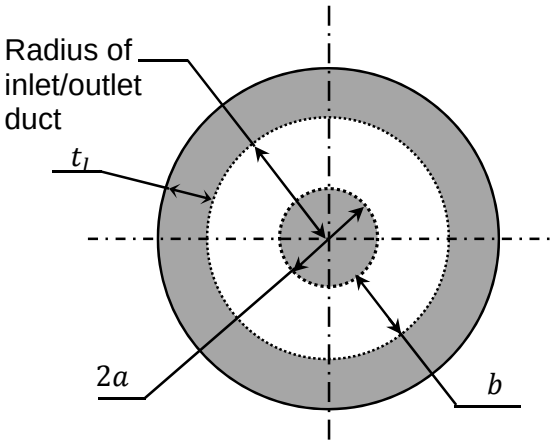

Figure 2a: Circular “pod” (CDM) splitter silencer

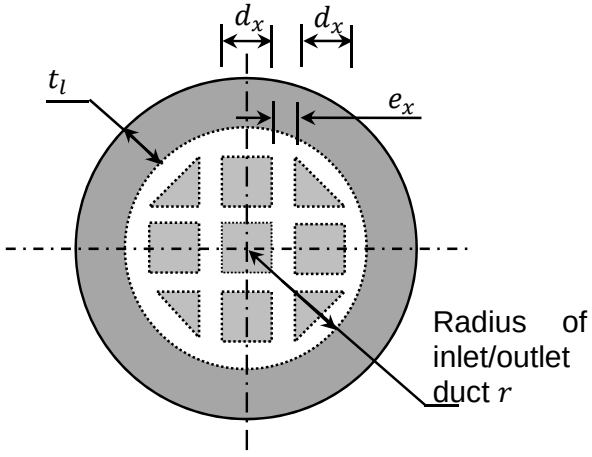

Figure 2b: Circular “bar” (CMDM) splitter silencer

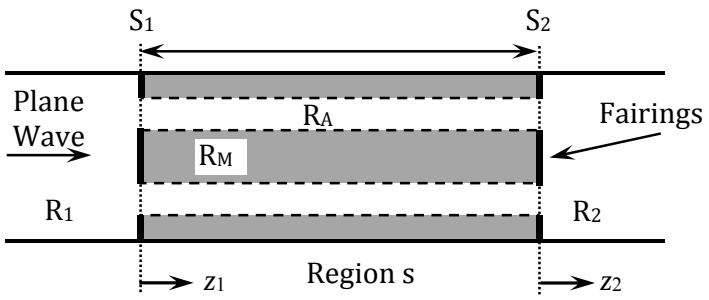

Figure 3. Geometry of uniform silencer.

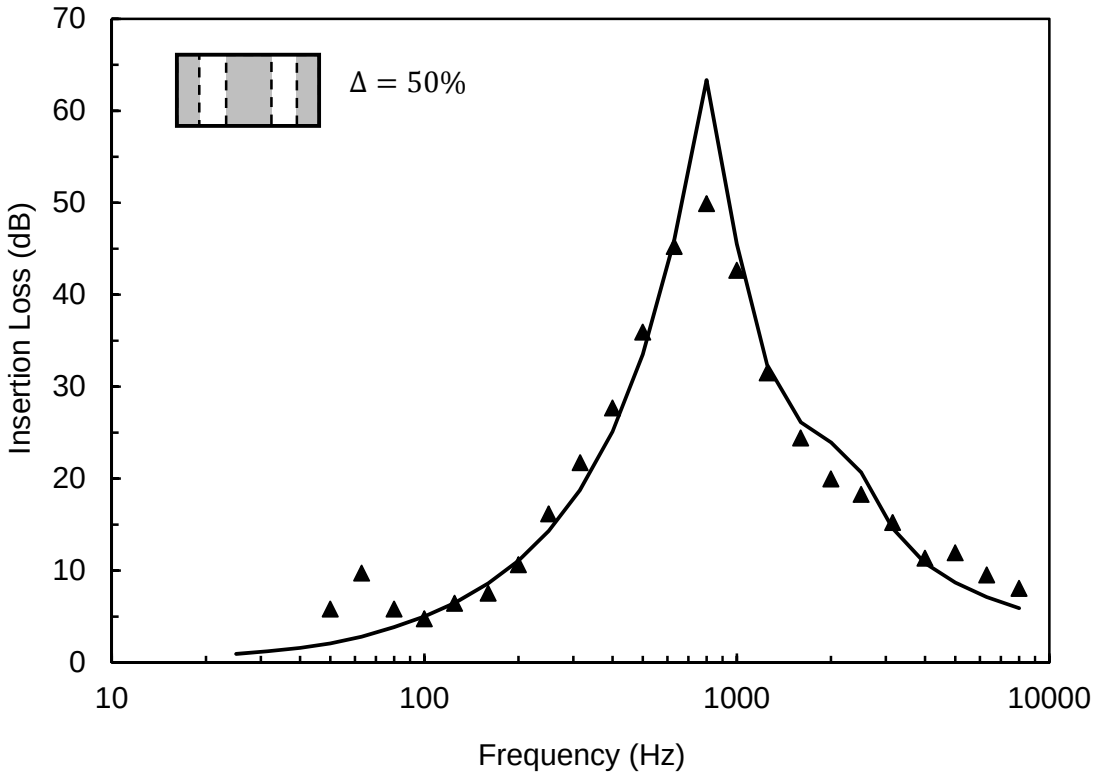

Figure 4. Measured and predicted IL for silencer SDM 1. ——, prediction; ▲ , measurement.

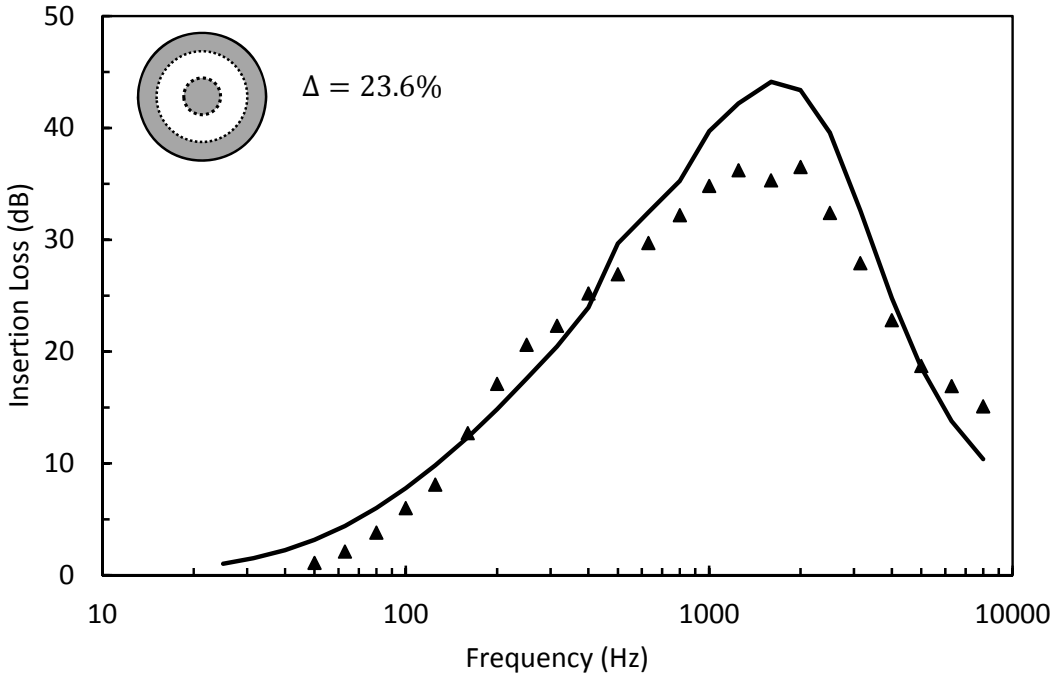

Figure 5. Measured and predicted IL for silencer TDM 1. ——— , prediction; ▲ , measurement.

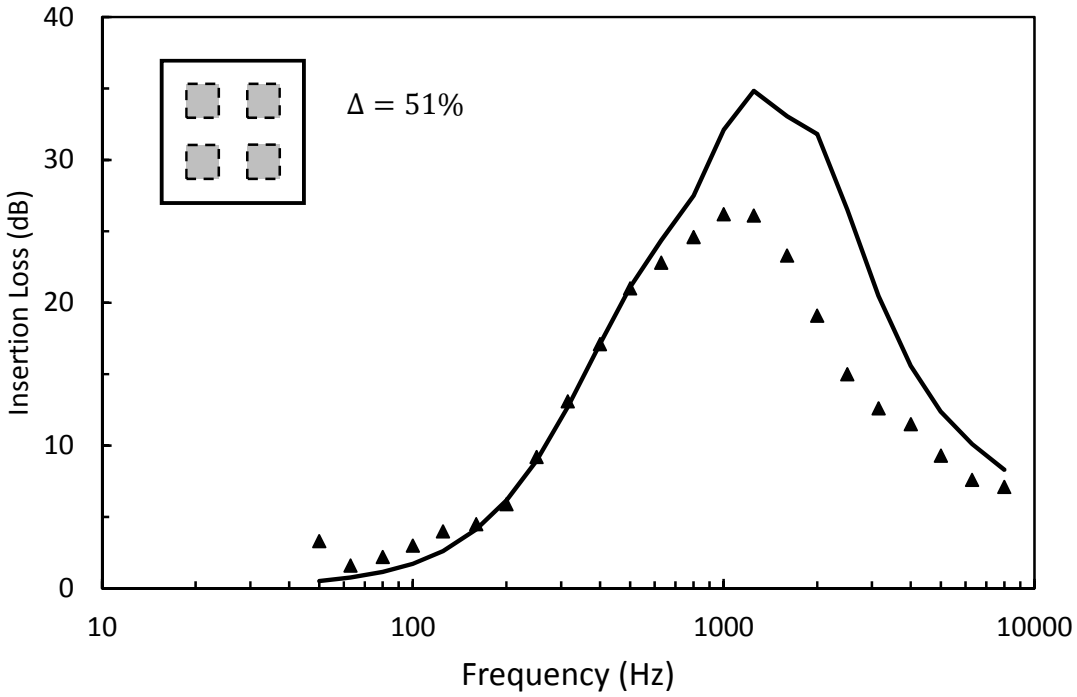

Figure 6. Measured and predicted IL for silencer MDM 1. ——— , prediction; ▲ , measurement.

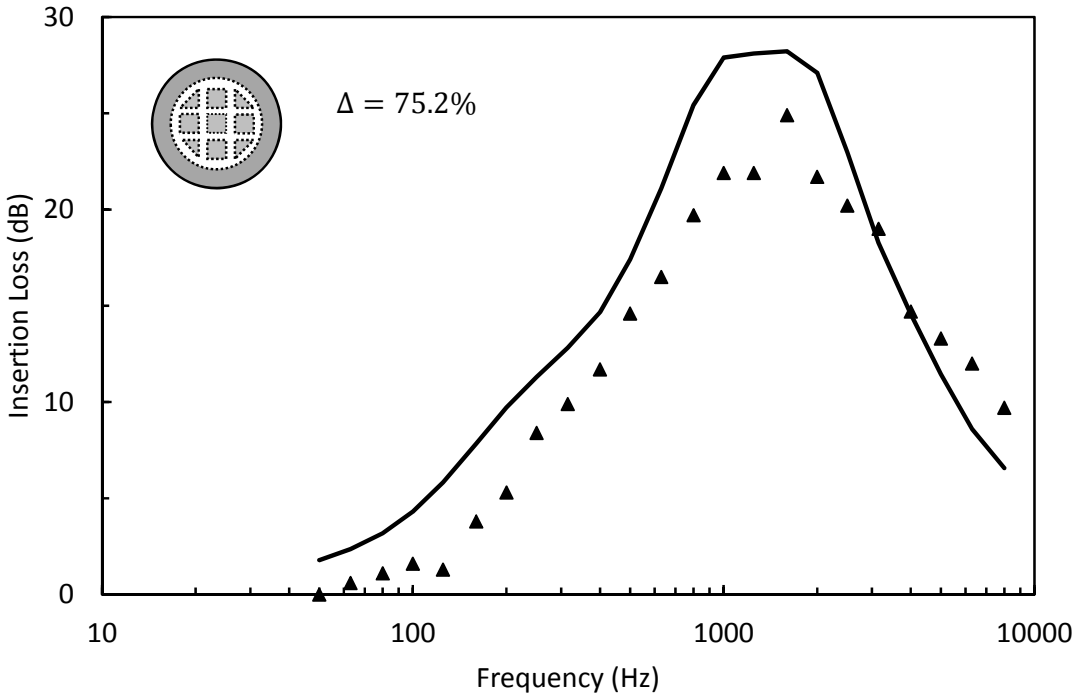

Figure 7. Measured and predicted IL for silencer CMDM 1. ——— , prediction; ▲ , measurement.

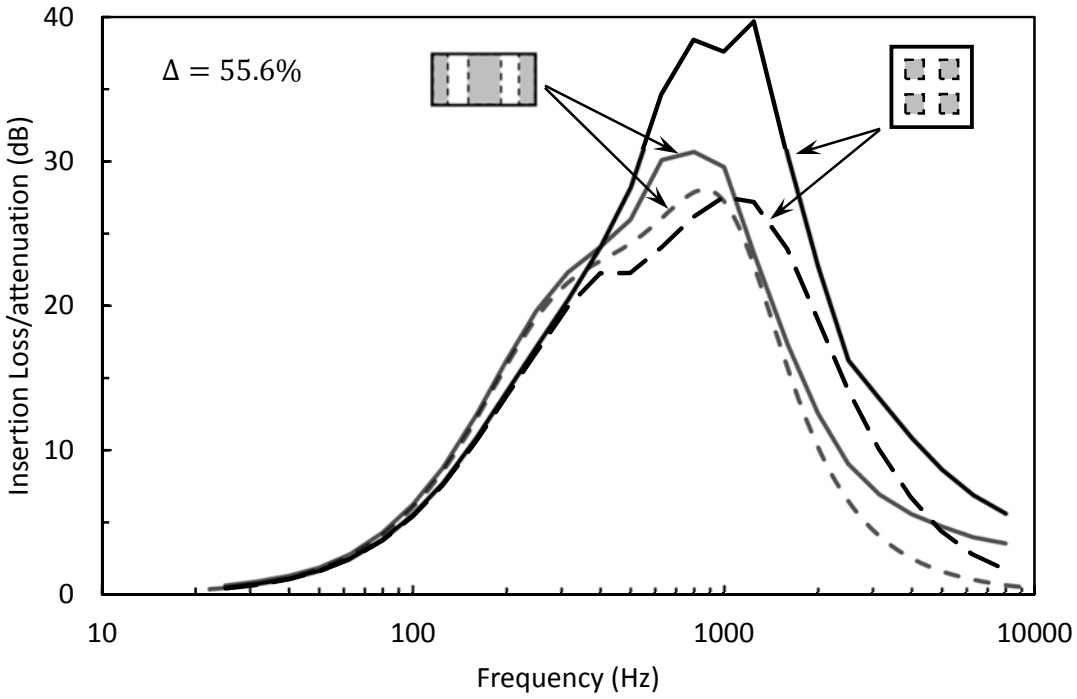

Figure 8. Predictions for Cummings and Astley silencer [16]. ———, IL SDM; ———, IL MDM; - - - - -, attenuation SDM; ; — — —, attenuation MDM

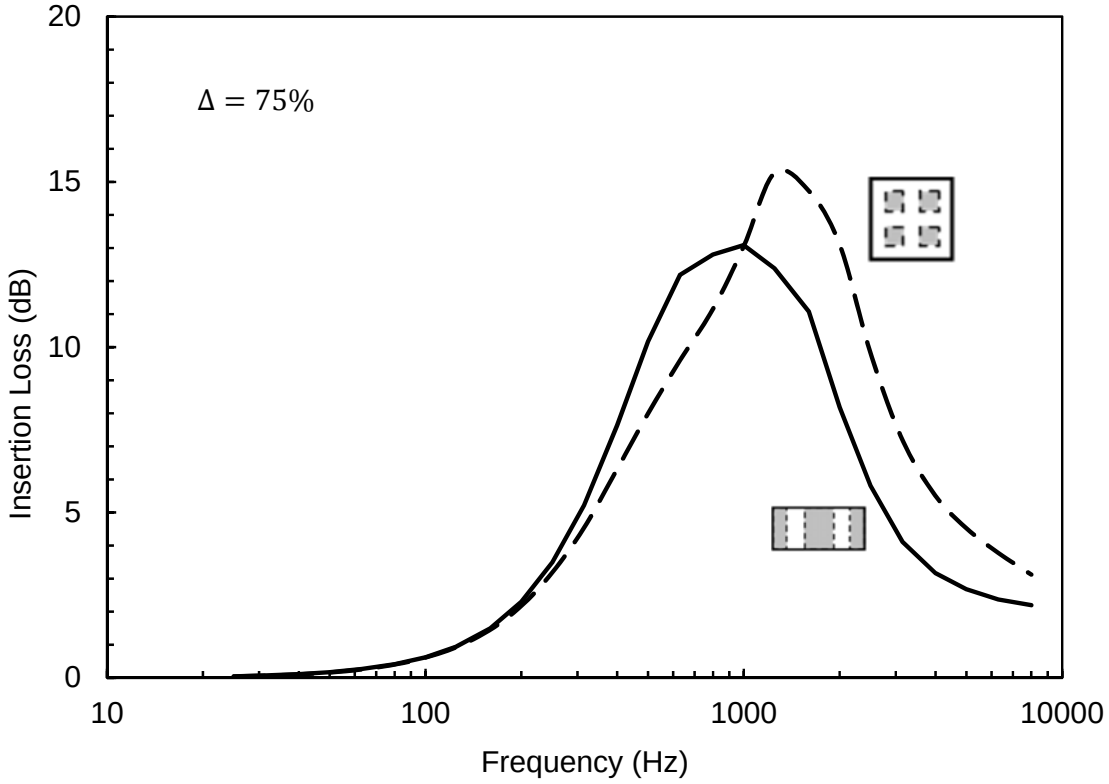

Figure 9a. Predicted IL for Δ = 75%. ——— , SDM 2; — — —, MDM 2 .

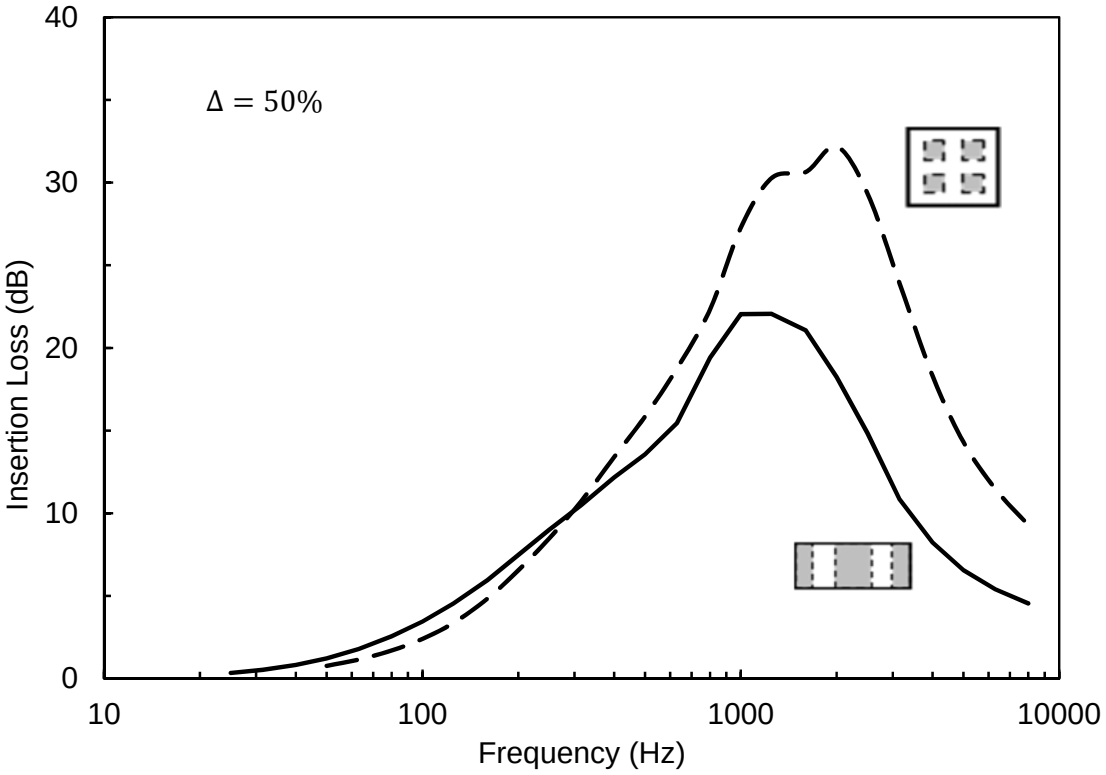

Figure 9b. Predicted IL for Δ = 50%. ——— , SDM 3; — — —, MDM 3 .

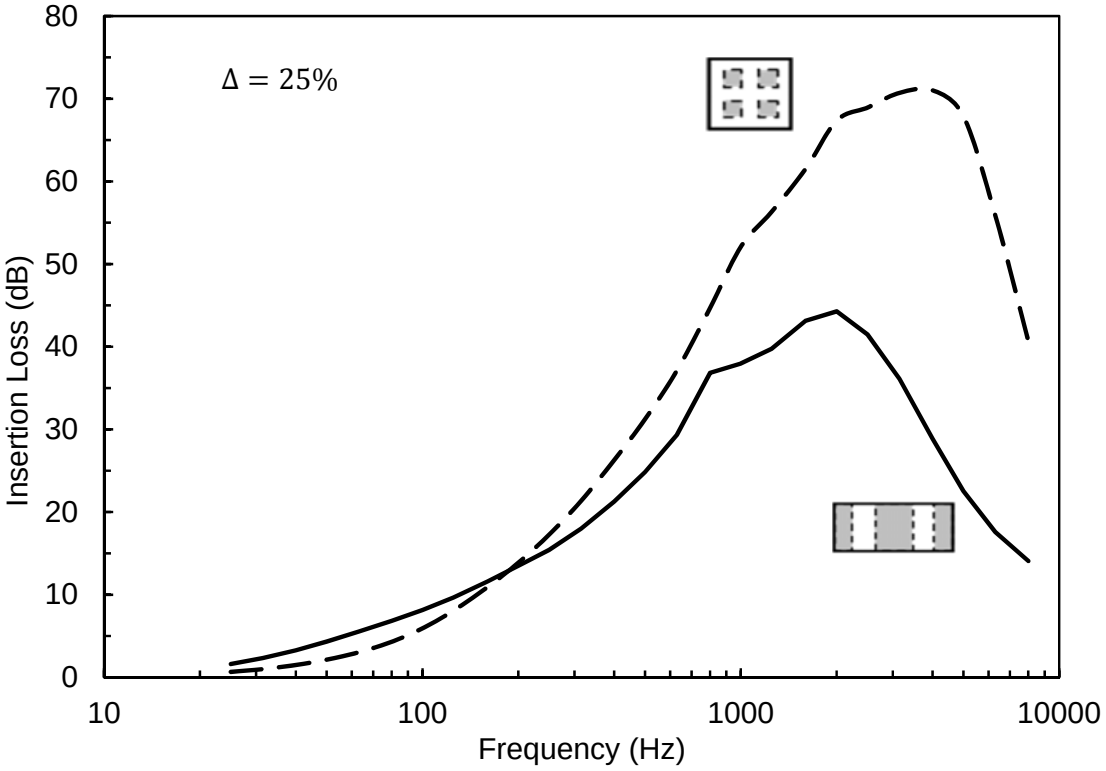

Figure 9c. Predicted IL for Δ = 25%. ——— , SDM 4; — — —, MDM 4 .

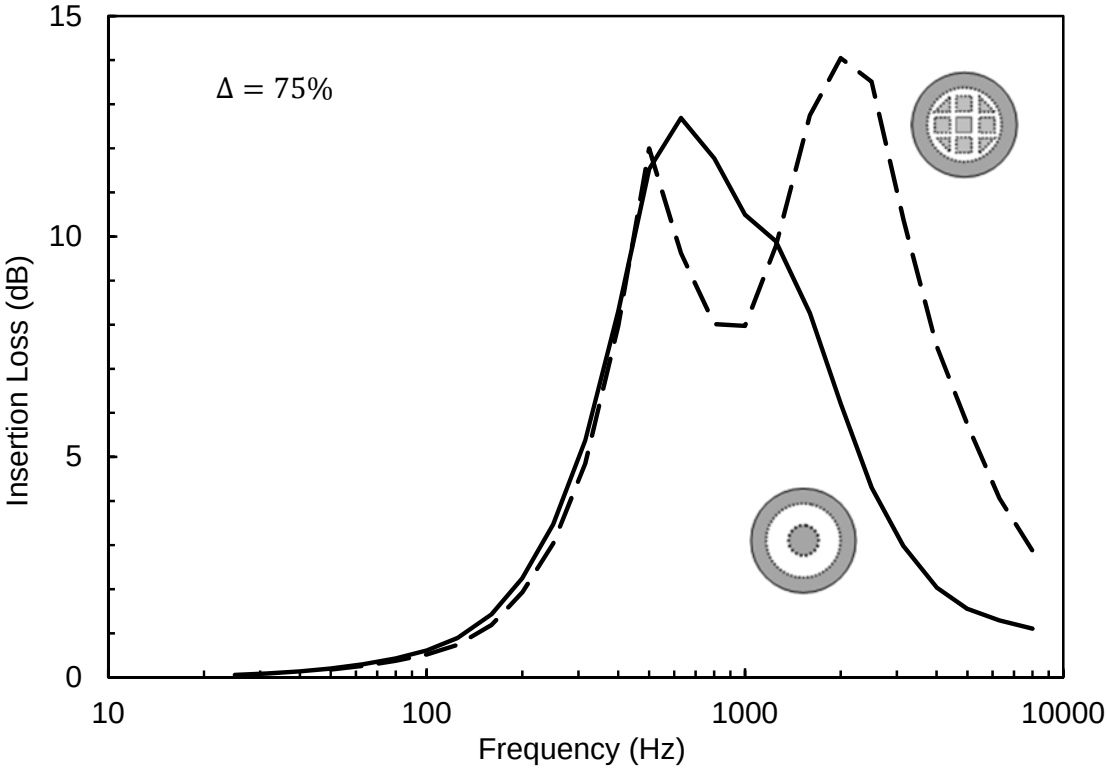

Figure 10a. Predicted IL for Δ = 75%. ——— , TDM 2; — — —, CMDM 2 .

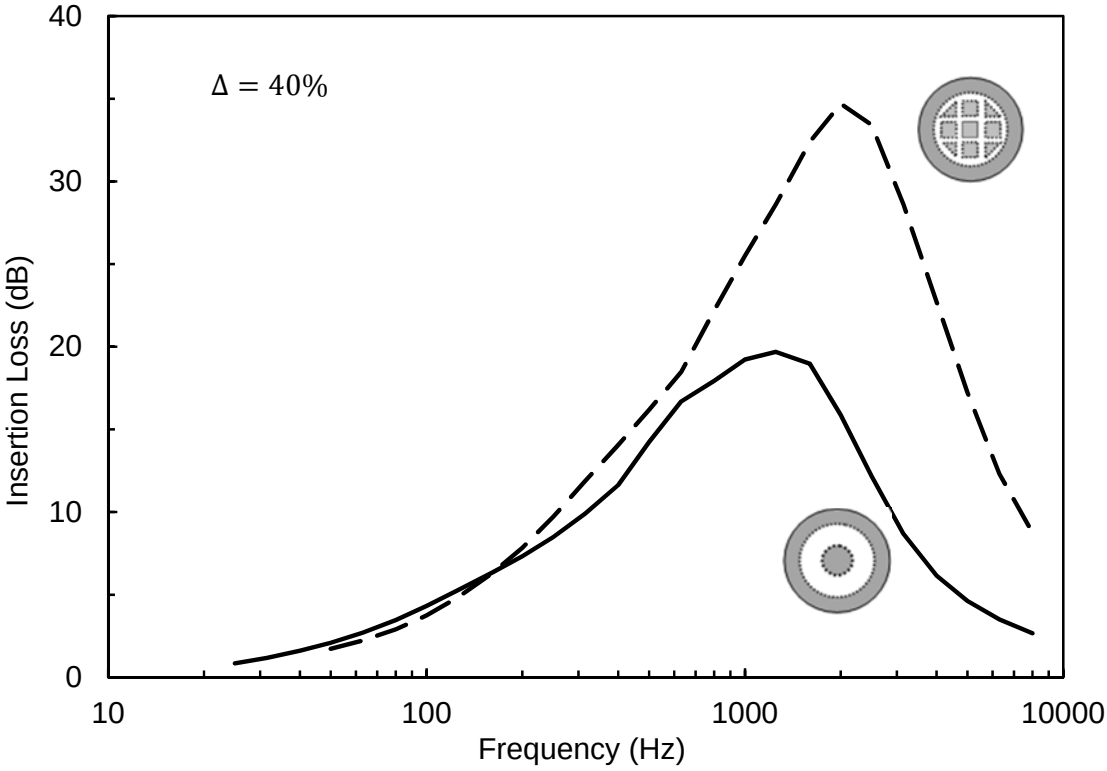

Figure 10b. Predicted IL for Δ = 50%. ——— , TDM 3; — — —, CMDM 3 .

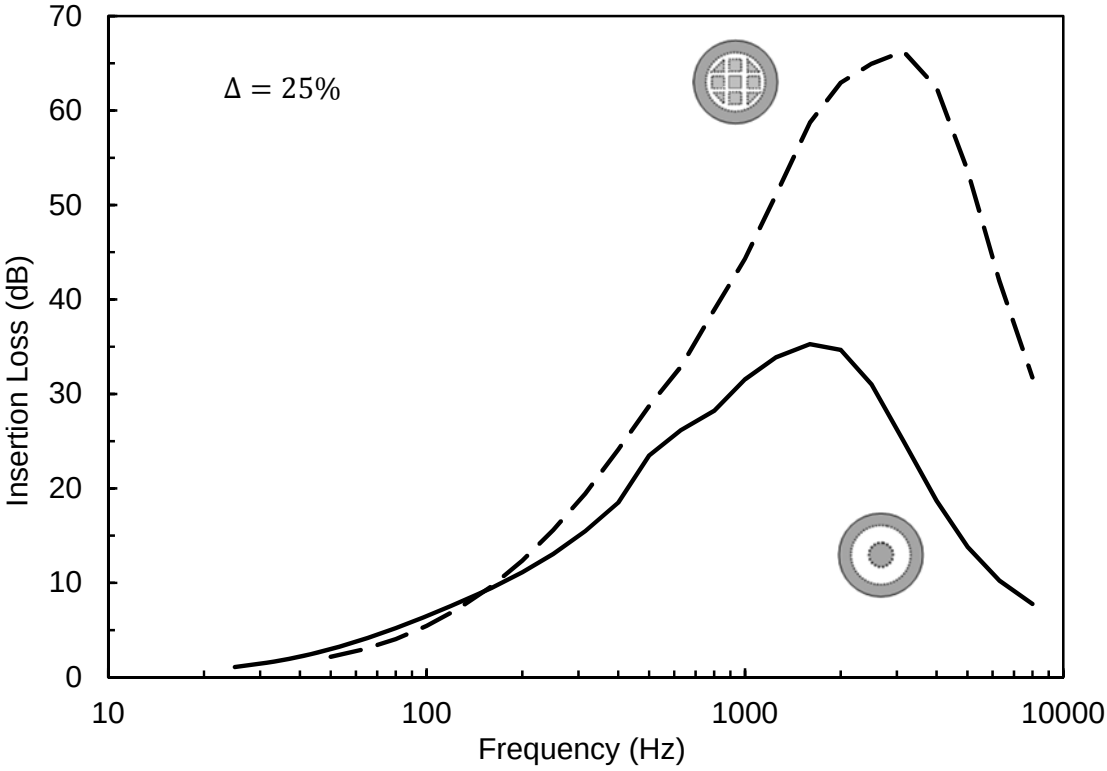

Figure 10c. Predicted IL for Δ = 25%. ——— , TDM 4; — — —, CMDM 4 .

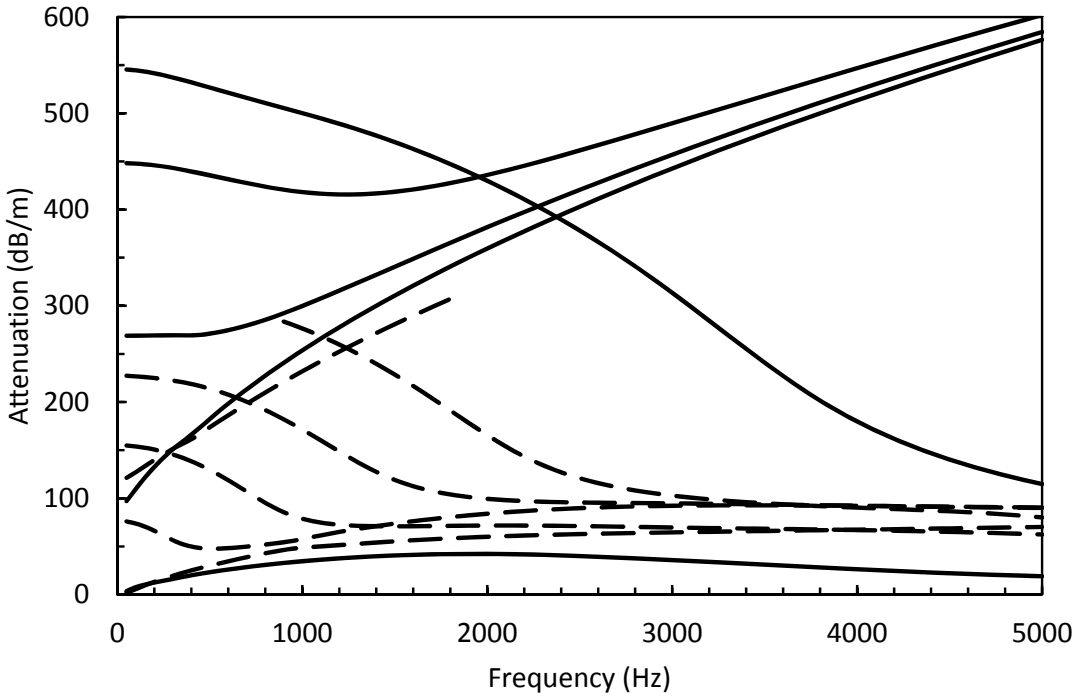

Figure 11. Predicted attenuation of the first five least attenuated modes.

———, SDM 4; — — —, MDM 4.